

Evaluating Semi-Analytic Halo Merging Histories

Rachel S. Somerville^{1,2}, Gerard Lemson^{1,3}, Tsafir S. Kolatt² and Avishai Dekel¹

¹*Racah Institute of Physics, The Hebrew University, Jerusalem*

²*Physics Department, University of California, Santa Cruz*

³*Max-Planck Institut für Astrophysik, Garching*

19 March 2021

ABSTRACT

We evaluate the accuracy of semi-analytic merger-trees by comparing them with the merging histories of dark-matter halos in N -body simulations, focusing on the *joint distribution* of the number of progenitors and their masses. We first confirm that the halo mass function as predicted directly by the Press-Schechter (PS) model deviates from the simulations by up to 50% depending on the mass scale and redshift, while the *means* of the projected distributions of progenitor number and mass for a halo of a given mass are more accurately predicted by the Extended PS model. We then use the full merger trees to study the joint distribution as a function of redshift and parent-halo mass. We find that while the deviation of the mean quantities due to the inaccuracy of the Extended PS model partly propagates into the higher moments of the distribution, the merger-tree procedure does not introduce a significant additional source of error. In particular, certain properties of the merging history such as the mass ratio of the progenitors and the total accretion rate are reproduced quite accurately for galaxy sized halos ($\sim 10^{12} M_{\odot}$), and less so for larger masses. We conclude that although there could be $\sim 50\%$ deviations in the absolute numbers and masses of progenitors and in the higher order moment of these distributions, the *relative* properties of progenitors for a given halo are reproduced fairly well by the merger trees. They can thus provide a useful framework for modelling galaxy formation once the above-mentioned limitations are taken into account.

Key words: galaxies: clustering – galaxies: formation – cosmology: theory – dark matter

1 INTRODUCTION

In the standard picture of hierarchical structure formation, small objects form first and then merge together to form larger objects as time progresses. Hierarchical structure formation is a generic prediction of the Cold Dark Matter (CDM) family of models, being a natural consequence of the general shape of the power spectrum. The process of structure formation can be represented by the “merging history” of virialized dark matter halos, i.e. the masses of the halos, identified at an earlier time when they were still distinct entities, that will later merge together to form a larger halo. This merging history is often referred to as a “merger tree”. This whole conceptual framework is somewhat artificial, relying as it does on a definition of “halo”, which involves assumptions of sphericity, virialization, etc. These properties almost certainly do not apply to all of the objects in the real universe that we might like to study. However, one reason for its popularity is that it enables one to develop analytic and semi-analytic predictions for many quantities of interest.

For example, the model developed by Press & Schechter

(1974) provides a simple but relatively effective framework for the description of the mass history of particles in a hierarchical universe with Gaussian initial perturbations. The original Press-Schechter (PS) model predicted the mass function of halos as a function of redshift, i.e. the number density of halos of a given mass at a redshift z . This prediction has been tested against the results of N -body simulations in several previous papers (Efstathiou et al. 1988; Gelb & Bertschinger 1994; Lacey & Cole 1994; Ma 1996; Tozzi & Governato 1997; Gross et al. 1998; Tormen 1998). The Press-Schechter theory was extended to give the *conditional* probability that a particle in a halo of mass M_0 at z_0 was in a halo of mass M_1 at an earlier redshift z_1 , leading to an expression for the conditional halo mass function (Bond et al. 1991; Bower 1991). This extended Press-Schechter (EPS) formalism can also be manipulated to obtain expressions for halo survival times, formation times, and merger rates (Lacey & Cole 1993, hereafter LC93). The extended Press-Schechter model and its implications have not been quite as well studied as the standard PS model, but Lacey & Cole (1994) and

arXiv:astro-ph/9807277v1 28 Jul 1998

recently Tormen (1998) have presented comparisons of the EPS model with N -body simulations.

However, the EPS formalism only provides us with *mean* quantities. In order to construct realizations of individual dark matter halo merging histories, one must include some additional assumptions. Although several methods for constructing merger trees have been proposed (Cole & Kaiser 1988; Kauffmann & White 1993; Somerville & Kolatt 1998), all of them involve some ad hoc ingredients. Such a method should be designed to reproduce both the conditional mass function predicted by the EPS model and to enforce conservation of mass at every stage. However, these constraints are not necessarily consistent with one another. This leads to certain ambiguities and subtleties in the process of constructing the merging trees, which we will discuss later in this paper. For a fuller discussion of these issues, however, see Somerville & Kolatt (1998, hereafter SK).

These merger trees form the framework for semi-analytic models of galaxy formation such as those described by Kauffmann, White, & Guiderdoni (1993), Cole et al. (1994), and Somerville & Primack (1998). The properties of the galaxies created in these models presumably depend to some degree on the merging history of the dark matter halos. Most of the previous work using the semi-analytic models has focussed on reproducing or predicting mean quantities and qualitative trends. However, it would be useful to investigate whether the broader properties of the predicted *distribution* of model galaxies are consistent with observations. For example, we might wish to investigate the scatter in well known observational relations like the luminosity-linewidth relation, the color-magnitude relation, or fundamental plane relations. But before we can trust the models for evaluating these kinds of questions, we must make sure that the merger trees not only satisfy the mean properties readily predicted by the EPS model, but ideally also the full distribution function. This has not been thoroughly investigated in previous work on this subject, and is the primary goal of this paper. The PS and EPS formalism do not provide any information about this distribution. Therefore we are forced to appeal to N -body simulations.

In this paper, we present a comparison between N -body simulations and semi-analytic merger trees (SAM-trees), as well as the analytic predictions of the EPS theory when they apply. We address several issues. First, we re-examine the agreement of the direct predictions of the standard and extended Press-Schechter model with the simulations. Although much of the previous work on this topic has stressed the unexpectedly good agreement, we focus on the discrepancies, their broader implications, possible causes and potential resolutions. We then study the success of the merger-tree method in the reconstruction of the distribution of progenitor number and mass compared to the results of the simulations, and examine several statistics relevant to the study of galaxy formation in a hierarchical context.

The outline of the paper is as follows. In §2, we give a brief summary of the PS and EPS formalism. In §3, we summarize the merger-tree method. In §4, we describe the N -body simulations. In §5, we present the comparison between the simulations and the SAM-trees. We discuss our results and conclude in §6.

2 THE PRESS-SCHECHTER FORMALISM

Suppose that we have smoothed the initial density distribution on a scale R using some spherically symmetric window function $W_M(r)$, where $M(R)$ is the average mass contained within the window function. There are various possible choices for the form of the window function (c.f. Lacey & Cole 1993). We use a real-space top-hat window function, $W_M(r) = \Theta(R - r)(4\pi R^3/3)^{-1}$, where Θ is the Heaviside step function. In this case $M = 4\pi\rho_0 R^3/3$, where ρ_0 is the mean mass density of the universe. The mass variance $S(M) \equiv \sigma^2(M)$ may be calculated from

$$\sigma^2(M) = \frac{1}{2\pi^2} \int P(k)W^2(kR)k^2 dk, \quad (1)$$

where $P(k)$ is the power spectrum of the matter density fluctuation, and $W(kR)$ is the Fourier transform of the real space top-hat.

The ‘‘excursion set’’ derivation due to Bond et al. (1991) leads naturally to the extended Press-Schechter formalism. The smoothed field $\delta(M)$ is a Gaussian random variable with zero mean and variance S . The value of δ executes a random walk as the smoothing scale is changed. Adopting an ansatz similar to that of the original Press-Schechter model, we associate the fraction of matter in collapsed objects in the mass interval $M, M + dM$ at time t with the fraction of trajectories that make their *first upcrossing* through the threshold $\omega \equiv \delta_c(t)$ in the interval $S, S + dS$. This may be translated to a mass interval through equation (1). The threshold $\delta_c(t)$ corresponds to the critical density at which a perturbation will separate from the background expansion, turn around, and collapse. It is extrapolated using linear theory, $\delta_c(t) = \delta_{c,0}/D_{\text{lin}}(z)$, where $D_{\text{lin}}(z)$ is the linear growth function (Peebles 1980). The halo mass function (here in the notation of LC93) is then:

$$f(S, \omega) dS = \frac{1}{\sqrt{2\pi}} \frac{\omega}{S^{3/2}} \exp\left[-\frac{\omega^2}{2S}\right] dS. \quad (2)$$

The *conditional* mass function, the fraction of the trajectories in halos with mass M_1 at z_1 that are in halos with mass M_0 at z_0 ($M_1 < M_0$, $z_0 < z_1$) is

$$f(S_1, \omega_1 | S_0, \omega_0) dS_1 = \frac{1}{\sqrt{2\pi}} \frac{(\omega_1 - \omega_0)}{(S_1 - S_0)^{3/2}} \exp\left[-\frac{(\omega_1 - \omega_0)^2}{2(S_1 - S_0)}\right] dS_1. \quad (3)$$

The probability that a halo of mass M_0 at redshift z_0 had a progenitor in the mass range $(M_1, M_1 + dM_1)$ is given by (LC93):

$$\frac{dP}{dM_1}(M_1, z_1 | M_0, z_0) dM_1 = \frac{M_0}{M_1} f(S_1, \omega_1 | S_0, \omega_0) \left| \frac{dS}{dM} \right| dM_1, \quad (4)$$

where the factor M_0/M_1 converts the counting from mass weighting to number weighting.

We can now derive two more quantities that will be useful later. Given the mass of a parent halo M_0 and the redshift step $z_0 \rightarrow z_1$, the *average* number of progenitors with mass larger than M_1 is:

$$\bar{N} \equiv \langle N_p(M | M_0) \rangle = \int_{M_1}^{M_0} dM \frac{M_0}{M} \frac{dP}{dM}(M, z_1 | M_0, z_0). \quad (5)$$

We can also readily calculate the average fraction of M_0 that dwelt in the form of progenitor halos of mass $M > M_l$:

$$\bar{f}_p = \int_{M_l}^{\infty} dM \frac{dP}{dM}(M, z_1 | M_0, z_0), \quad (6)$$

and define the complimentary quantity for the average fraction of M_0 that came from “accreted” mass, $\bar{f}_{acc} = 1 - \bar{f}_p$.

Throughout this paper we use the standard value for the collapse threshold, $\delta_{c,0} = 1.69$, corresponding to the value predicted by the top-hat spherical collapse model.

3 THE TREES

We first should clarify some of our terminology. Suppose we have identified a halo of a given mass at some redshift, whose merging history we wish to know. This halo is referred to as the “parent”. We then go backwards in time and trace all the smaller halos that merged together in order to form this halo. These are referred to as “progenitors”. Although it violates the usual temporal relation of kinship, because we construct the tree working backwards in time, this has become the usual terminology.

Let us suppose that we set out to construct a merger tree, taking the EPS formalism as an ansatz. Such a merger tree should satisfy at least two basic requirements: each individual halo history should conserve mass at every stage, and the EPS and PS mass functions (for every redshift) should be reconstructed in the mean for a large ensemble of realizations. Unfortunately, satisfying both requirements exactly and simultaneously is not straightforward, and is sometimes impossible for certain choices of power spectrum and redshift interval. There are also additional problems – the EPS formalism gives us the *single* halo probability that a halo with mass M_0 at z_0 has a progenitor of mass M_1 at z_1 — it does not provide us with any information about the rest of the progenitors that make up the mass of M_0 (i.e. the *joint* progenitor probability function). There are certain obvious constraints which the EPS formalism knows nothing about, for example, the sum of the progenitor masses clearly cannot exceed M_0 . In addition, since the number of halos diverges at very small mass, one must impose some minimum mass M_l , below which one no longer follows the history of these halos. However, one must account for the mass contributed by these small halos. We will refer to halos with masses larger than M_l as “progenitors”, and the mass contributed by halos smaller than this limit as “accreted mass”.

One must therefore form a compromise between mass conservation and reconstructing the mean as predicted by the EPS model, and one must make some ad-hoc assumptions in order to fill in the gaps mentioned above. In the method of Kauffmann & White (1993), the mean progenitor mass distribution is reproduced exactly, and mass conservation is enforced only approximately. In the scheme of Somerville & Kolatt (1998), mass conservation is enforced exactly and the mean progenitor distribution is reproduced approximately.

We now sketch the method of SK. Given a parent halo with mass M_0 , the histories of individual particles, or trajectories, in the language of the excursion set formalism, are followed back in time using very small timesteps. For each particle that finds itself in M_0 at z_0 , we choose the mass

of the progenitor halo it was located in at an earlier redshift z_1 from Eqn. 3. A “branch” occurs when at least two trajectories are found in halos with masses greater than the minimum halo mass M_l . The timestep has been chosen such that “branching” events are improbable; i.e. in most cases one trajectory will be in a halo with mass close to M_0 and others will be in halos with masses less than M_l . This ensures that most of the branching events involve small numbers of branches, but no limit is imposed on the number of branches allowed. In order to avoid choosing a progenitor with a mass larger than the remaining unallocated mass, the probability function is truncated for masses larger than this value. The contribution from “accreted mass” is included explicitly from trajectories that find themselves in halos smaller than M_l . It is possible to include these without introducing a large computational overhead because the *mass weighted* probability, used for the trajectories, does not diverge at small mass. One continues to follow trajectories until all of the mass of the parent has been accounted for. Therefore mass is conserved exactly. However, the shape of the conditional mass function that is obtained, although very similar to the EPS prediction we wish to reconstruct, is not exact (see SK).

4 THE SIMULATIONS

In order to study the formation histories of halos in numerical simulations, we need:

- (i) High mass and force resolution
- (ii) A large enough volume to contain many halos in the mass range of interest
- (iii) Stored data for several time steps, at appropriate redshifts.

We use the adaptive particle-particle/particle-mesh simulations of the VIRGO consortium (Jenkins et al. 1997). The resolution and box size of the smaller volume simulations in the suite are appropriate for our purposes, since we wish to focus on galaxy or group sized halos.

We present our results for the τ CDM model, a critical ($\Omega = 1$) model with shape parameter $\Gamma = 0.21$. This value of the shape parameter is motivated by observations of galaxy clustering (Maddox et al. 1990; Maddox, Efstathiou, & Sutherland 1996; Vogeley et al. 1992). The parameters of the simulation are given in Table 1. We have performed the same analysis for a simulation with $\Omega_0 = 0.3$ and an open geometry, and we find qualitatively similar results to those we will describe for the τ CDM model, leading to similar conclusions. We therefore do not present the results from other cosmological models.

The halos are identified using a standard “friends-of-friends” algorithm with a linking length $b = 0.2\bar{d}$, where \bar{d} is the mean interparticle spacing $\bar{d} = L_{\text{BOX}}/256$. The friends-of-friends algorithm with this value for the linking length has been shown to give roughly equivalent results to spherical over-density based halo finders (Lacey & Cole 1994).

The procedure to identify progenitors and assign their masses is as follows. Consider a parent halo with mass M_0 at $z = 0$. We track each particle in this halo to an earlier redshift, z_1 , and find the mass of the halo in which it is located at that time. We then identify all the other particles

Table 1. Simulation Parameters. From left to right, the quantities given are the mass density in units of the critical density, the Hubble parameter $h \equiv H_0/(100 \text{ km s}^{-1} \text{ Mpc}^{-1})$, the linear rms mass variance on a scale of $8h^{-1} \text{ Mpc}$, the number of particles, the number of grid cells, the length of one side of the box, and the mass per particle.

Model	Ω_0	h	σ_8	N_p	N_g	L_{box} (Mpc)	m_p (M_\odot)
τ CDM	1.0	0.5	0.6	256^3	512	170	2.0×10^{10}

in the progenitor halo that are also present in the parent halo M_0 at $z = 0$. At this point, we may be faced with several problems which reflect the inconsistency of the simple merging hierarchy picture with the numerical properties of N -body simulations. We may encounter the unphysical situation where a progenitor halo identified in this way has a mass larger than the parent. This is simply because individual particles are often stripped or ejected from halos in the simulations. If this occurs, we exclude the parent halo from our sample. In addition, not all the particles in the progenitor end up in the same parent halo. We then have two possible choices of ways to assign mass to the progenitor. We can either take only the mass of all the particles in the progenitor that also end up in the parent halo, or we can take the total mass of the progenitor halo. In the first case, the mass does not reflect the dynamical mass of the progenitor, which is the quantity that is treated by the PS formalism. In the second case, conservation of mass is violated. Since it is not clear which is the most consistent prescription, and since these two choices in some sense represent opposite extremes, we have performed our analysis using both schemes. We shall refer to the masses identified in these two ways as the “inclusive” (mass of particles that end up in parent) and “total” (total virial mass of progenitor) progenitor masses.

Recall that in the SAM-tree procedure, we defined a minimum progenitor mass M_l . In the case of the trees, this mass scale is arbitrary, but in the simulations, we should choose it to correspond to the smallest halo that we believe to be numerically stable. We have tried using a minimal halo mass corresponding to both 10 and 25 particles. We show the results for the choice of 25 particles because the agreement between Press-Schechter and the simulations is better, and because the results for the two different definitions of progenitor mass discussed above are more consistent with one another. This leads us to believe that the results are less affected by the numerical instability of the halos if we only consider halos of more than 25 particles. As in the trees, we now term the total amount of mass contributed by halos with masses smaller than M_l as the “accreted mass”. The estimate of the accreted mass also depends on the method used to assign progenitor masses. For the “inclusive” scheme, the mass of the halo is more likely to fall below M_l and hence the estimate of accreted mass tends to be larger.

5 THE COMPARISON

5.1 Mean Quantities

In this section, we compare the results of the simulations described in the last section with the predictions of the PS and EPS models, and with the results of the SAM-trees described in §3. In the remainder of the paper, we

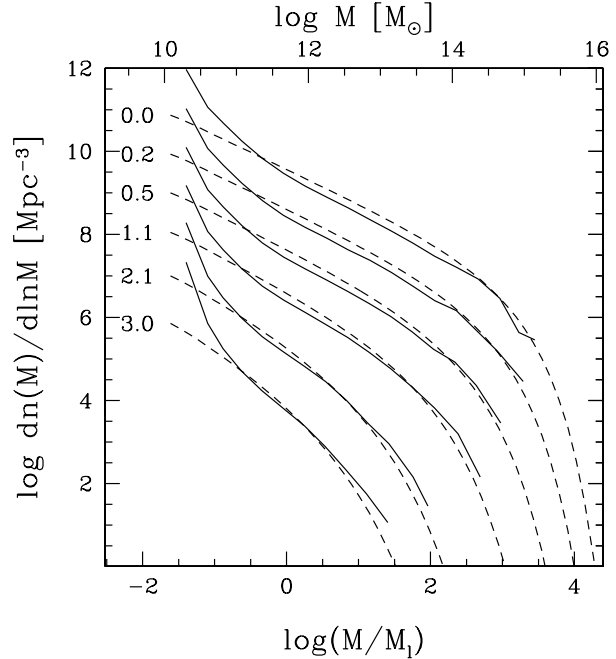


Figure 1. The mass function of halos predicted by the standard Press-Schechter model (dashed lines), and found in the simulations (solid lines) at redshifts of (from top to bottom) $z = 0, 0.2, 0.5, 1.1, 2.1, \text{ and } 3.0$.

will express all masses in terms of the minimum progenitor mass, M_l , which here corresponds to a physical mass of $25 m_p = 5.0 \times 10^{11} M_\odot$. In order to have sufficient statistics, we group the parent halos in the simulations into ten logarithmically spaced mass bins, spanning the mass range from $5 M_l$ to $500 M_l$. We generate the SAM-trees for a grid of parent masses covering the range of M_0 in each mass bin used for the simulations, weighting the contribution according to the Press-Schechter number density at $z = 0$. This is an attempt to mimic the range of parent masses represented in a given bin in the simulations, and accordingly any scatter in the distributions that may result from this effect.

Figure 1 shows the overall halo mass function for the simulations, compared with the standard Press-Schechter model. At $z = 0$, the PS model agrees well with the simulations at high masses ($\gtrsim 10^{14} M_\odot$), and overpredicts the number of halos by about a factor of two between masses of 10^{14} and $\sim 5 \times 10^{11} M_\odot$. At very small masses ($\lesssim 2 \times 10^{11} M_\odot$), the simulations have many more halos than the PS model prediction, which is almost certainly due to numerical effects.

The scatter in the simulation mass function due to shot noise is insignificant on the mass scales where the discrep-

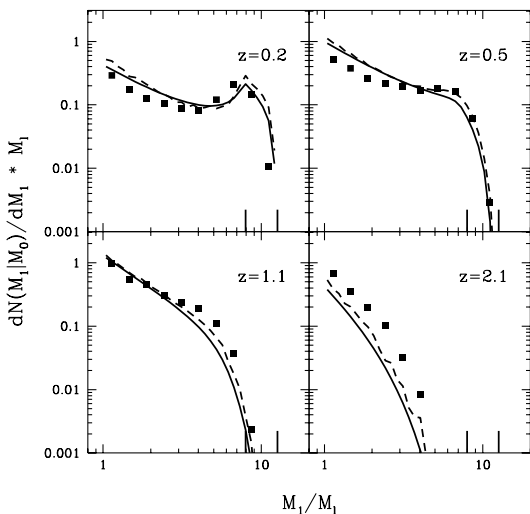


Figure 2. The conditional mass function of halos predicted by the Extended Press-Schechter model (solid lines), found in the simulations (filled squares), and in the SAM-trees (dashed lines). The Extended Press-Schechter prediction and the SAM-trees have been averaged over the bin in parent mass used for the simulations, indicated by the vertical lines on the bottom of the box. The panels show redshifts 0.2, 0.5, 1.1, and 2.1 as indicated on the figure. The mean parent mass is $\bar{M}_0 = 10M_l$.

any with the Press-Schechter model has been noted (at $z = 0$, less than 5 percent for $M \lesssim 10^{13}M_\odot$, less than 10 percent for $M \simeq 10^{14}M_\odot$). If plotted as error bars on Fig. 1, the width of the error bars on these scales would be about the same as the width of the line used to plot the mass function. The shot noise becomes significant (greater than 20 percent) only for the two largest mass bins ($M > 5 \times 10^{14}$), which contain only a few halos because of the limited volume of our simulation box.

The mass scale at which the PS model starts to underestimate the number of halos moves to smaller values with increasing redshift. This means that by a redshift of $z \sim 3$, the simulations have considerably more halos than the PS prediction at masses $\gtrsim 10^{12}M_\odot$; i.e. the evolution of the mass function with redshift is exaggerated in the PS model. However, the mass scale of the steepening on the small mass end remains constant with redshift, as expected if it is indeed due to numerical effects.

It should be noted that Gross et al. (1998) and Gross (1997) find the similar results (both the nature and magnitude of the discrepancy and its dependence on redshift) using a different kind of code (Particle-Mesh) and a different method for identifying halos (spherical and elliptical overdensity methods). The same results are obtained in all five of the CDM-variant cosmologies simulated by Gross et al. (1998). Similar results have also been obtained by Tormen (1998) and Tozzi & Governato (1997). It should also be noted that changing the value of the parameter $\delta_{c,0}$ will only cause the PS mass function to cross the simulation mass function at a different mass scale and cannot bring the mass functions into good agreement simultaneously on all scales.

Figure 2 shows the conditional mass function for a bin in parent halo mass $M_0 = 7.9\text{--}12.6 M_l$; i.e. the probability that the parent halo had a progenitor of mass M_l at some earlier redshift z_1 . The geometric mean parent mass is approximately $10 M_l$, which with our choice of $M_l = 5.0 \times 10^{11}$, corresponds to the mass of the halo surrounding an L_* galaxy ($M = 5.0 \times 10^{12}M_\odot$). In addition to being a relevant mass scale if we are interested in studying galaxy formation, there are many such halos in our simulation volume, so that shot noise is insignificant for the remainder of the comparisons that we shall discuss. Figure 2 shows the prediction of the EPS theory (Eqn. 4), the SAM-trees, and the results of the simulations. The EPS prediction and the SAM-trees have been averaged over the bin in parent halo mass used for the simulations. We find that the simulation results are reasonably similar for the two progenitor mass identification schemes described in Section 4, so we simply average the values obtained in the two schemes for the remainder of the paper.

Note that the discrepancy between the EPS theory and the simulations is qualitatively similar to the discrepancy that we saw before between the standard PS and the total mass function. The simulations have fewer halos than EPS in the intermediate mass range, and (though this is not shown in the figure) steepen at very small masses ($\lesssim M_l$). We also see the same reversal in the trend as a function of redshift. The peak near M_0 is moved to somewhat smaller masses. This means that the largest progenitor in the simulations is somewhat smaller than in the the EPS-based trees, and the complementary accreted mass is larger. Similar effects are seen for cluster-sized halos in the simulations of Tormen (1998).

5.2 Distributions

We now address the distribution of progenitor mass and number, i.e. the probability that a halo of mass M_0 at z_0 had a progenitor at z_1 with mass M_p , and that this progenitor was a member of a set of n progenitors. We denote this as $P(n, M_p)$. We show this distribution in figures 3–4. The number of points plotted in each bin is proportional to $P(n, M_p)$. We have offset the points randomly within the bins for clarity, although n can actually take only integer values. We show the results for parent halos in mass ranges centered on $\bar{M}_0 = 10 M_l$ and $\bar{M}_0 = 40 M_l$, for both the simulations and the SAM-trees. Note that the smaller mass parent corresponds to the mass of the dark matter halo surrounding an isolated L_* galaxy, and the larger mass parent to the dark matter halo surrounding a group.

These distributions show qualitatively the same behaviour for the SAM-trees and the simulations. At $z = 0.2$ most of the progenitors are single progenitors with masses close to that of the parent, with the rest of the mass coming from accretion (halos smaller than M_l). As we go back to progressively higher redshifts, the mean progenitor mass shifts towards smaller masses, but the mean number of progenitors stays roughly constant. With some imagination, one can see the shape of an elephant head in these plots: the wide roundish part on the left is the “head” and the curved plume extended out to the right is the “trunk” (especially noticeable in the larger mass parent halo shown (figure 4)). At low redshift, there is a clump of progenitors with mass close to

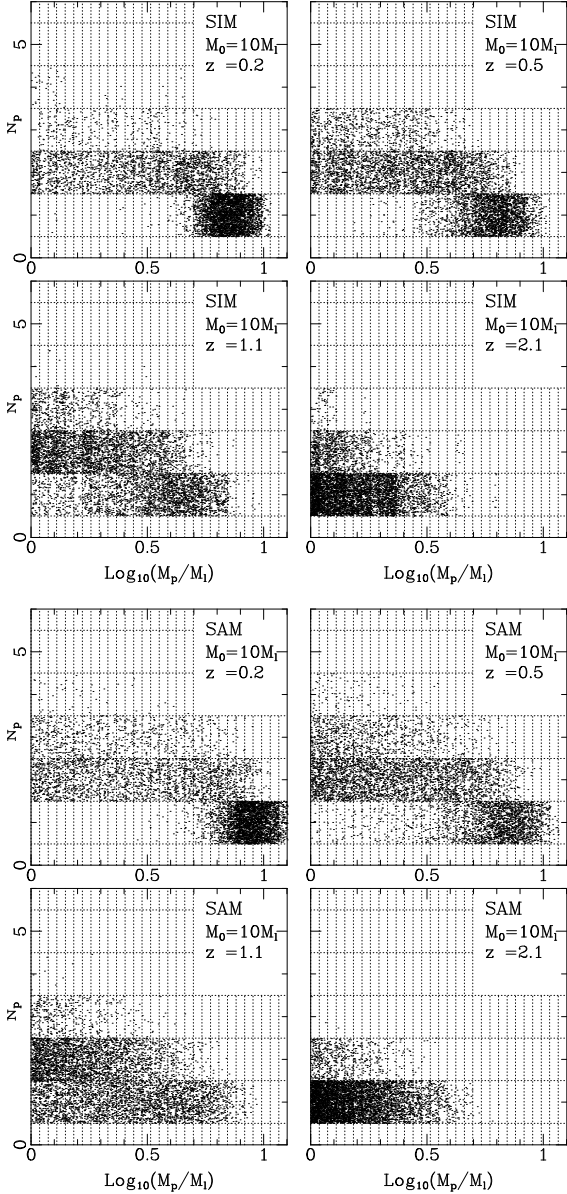


Figure 3. The two-dimensional distribution of the number of progenitors and their masses at redshifts 0.2, 0.5, 1.1, and 2.1, for parent halos with average mass $\bar{M}_0 = 10 M_1$. The points have been plotted with random offsets within the bins. The top panel shows the simulations, and the bottom panel show the SAM-trees.

M_0 and small numbers of progenitors, which broadens as it moves towards larger numbers of smaller progenitors. As we move to higher redshift, this clump at the end of the “trunk” drains further back into the “head”, and the trunk becomes less and less pronounced, until by $z = 2$ there is almost no trace of it. The “trunkiness” (i.e. the presence of the thin extended plume) persists longer (until higher redshift) for larger mass parents. Elephants with trunks correspond to a situation where halos are formed from several progenitors, and in this case we would expect to find several galaxies within a single dark matter halo. Elephants without trunks (the more rounded distributions) correspond to a situation where there is often a single progenitor that has

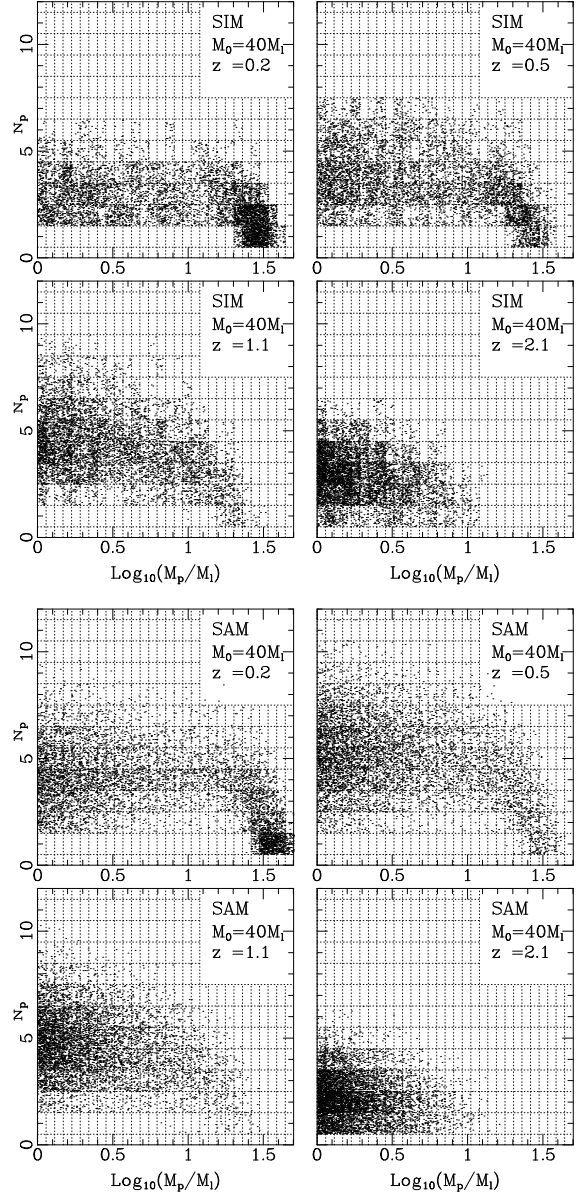


Figure 4. Same as figure 3 for $\bar{M}_0 = 40 M_1$.

mostly grown by accreting mass. Thus in a very general way, we can understand from these distributions how the merging history of an isolated L_* galaxy differs from one living within a group or cluster. This characteristic shape is a direct result of the combined constraint of the progenitor mass distribution (figure 2) and mass conservation. Thus any merger tree method that satisfies these constraints should reproduce the general properties of the mass-number distribution, regardless of the details of the method.

When we try to compare the distributions more stringently, we immediately notice several differences. In the first redshift interval, the SAM-trees have progenitors filling in all the mass bins up until the largest bin. This indicates that there are progenitors with masses very close to M_0 , which have accreted a very small amount of mass. In the simulations, the largest progenitor mass bins are almost empty. This is a reflection of the same discrepancy that we saw in

the conditional mass function (figure 2) — the peak in progenitor mass near M_0 was shifted towards smaller masses in the simulations. This means that the largest progenitor is smaller and the average accreted mass is larger in the simulations. Another, related difference in the $P(n, M_p)$ distributions is that in the SAM-trees, the “elephant head” is more diffuse and is shifted towards larger numbers of progenitors. The elephants also lose their trunks faster as one goes to higher redshift in the SAM-trees (indicating that the evolution is faster). This again mirrors what we saw in the conditional and overall mass functions: the simulations have more high-mass halos at high redshift than the EPS model predicts, indicating less evolution. These discrepancies become more and more noticeable for larger parent masses. We therefore see that the discrepancies in the mean quantities predicted directly by the PS and EPS theory compared with the simulations lead to discrepancies in the merging history of the halos obtained from the EPS-based SAM-trees.

The complement of the quantity presented above is the distribution of progenitor number and accreted mass, $P(n, f_{\text{acc}})$. This is the probability that a halo with mass M_0 had n progenitors and $f_{\text{acc}} \equiv M_{\text{acc}}/M_0$ in accreted mass. In figure 5, we indeed see a behaviour that is complementary to that we have just discussed with relation to the distribution $P(n, M_p)$. The fraction of the parent mass in the form of accreted mass is larger in the simulations, and there is less scatter in both f_{acc} and N_p than in the SAM-trees. The accreted mass increases as we move to higher redshift, reflecting the fact that a larger fraction of the mass in the universe is in the form of very small halos. The number of progenitors increases until a redshift of about $z = 1$, when the number decreases as more of the progenitors fall below the mass resolution.

5.3 Projections

The “trunk” plots discussed in the previous section provide a qualitative impression of the evolution of the distribution we are interested in, but they are somewhat difficult to interpret quantitatively. Note that the conditional mass function shown in §5.1, $P(M_p)$, is a projection of the distribution $P(n, M_p)$: $P(M_p) = \sum_n P(n, M_p)$. We can also look at the orthogonal projection, i.e. the probability of having n progenitors, regardless of their mass, $P(n) = \int_{M_l}^{M_0} P(n, M_p) dM_p$. We show this quantity for the simulations and the SAM-trees in figure 6.

The agreement of the distributions in the smaller mass bin, $M_0 = 10 M_l$ is quite good. For the larger mass bin, $M_0 = 40 M_l$, the trees are skewed towards *larger* numbers of progenitors at $z = 0.5$, agree almost perfectly with the simulations at $z = 1$, and are skewed in the opposite direction (towards smaller number of progenitors) at $z = 2$. The sense of these discrepancies and the reversal of the trend with redshift should be quite familiar by now and are a direct result of the discrepancies between the EPS model and the simulations that we have already remarked upon.

Similarly, the projection of the distribution $P(n, f_{\text{acc}})$ gives the probability that a fraction of the parent mass f_{acc} was in the form of accreted mass, regardless of the number of progenitors. This is shown in figure 7. Once again we can compare the EPS prediction for the mean value of f_{acc} , from

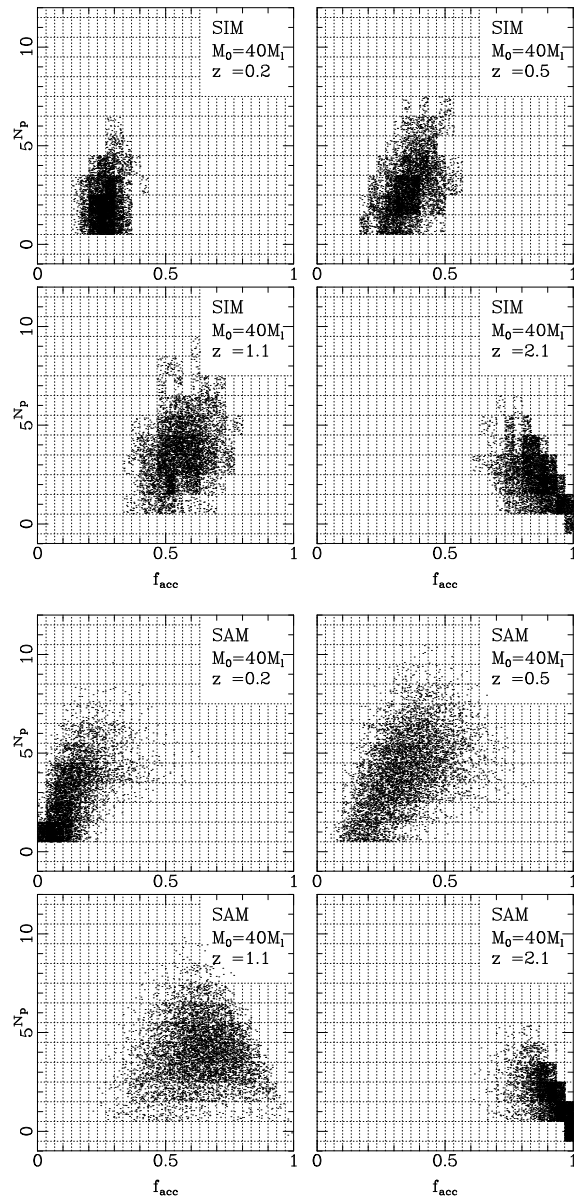


Figure 5. The two-dimensional distribution of the number of progenitors and the fraction of the parent mass in the form of accreted mass, at redshifts 0.2, 0.5, 1.1, and 2.1, for parent halos with average mass $\bar{M}_0 = 40 M_l$. The points have been plotted with random offsets within the bins. The top panel shows the simulations, and the bottom panel shows the SAM-trees.

equation 6, and shown on the figures by the full vertical line, with the means of the distributions in the simulations and the SAM-trees. The mean accreted mass in the simulations is larger than the EPS prediction at small redshift and smaller at higher redshift. This is once again a consequence of the original discrepancy mentioned above.

5.4 Moments

In figure 8, we show the first moment and rescaled second and third moments of the distribution of the number of progenitors P_n as a function of the parent halo mass, M_0 . The

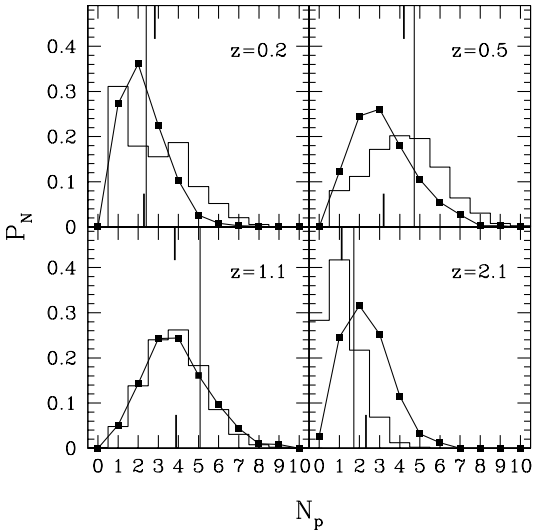
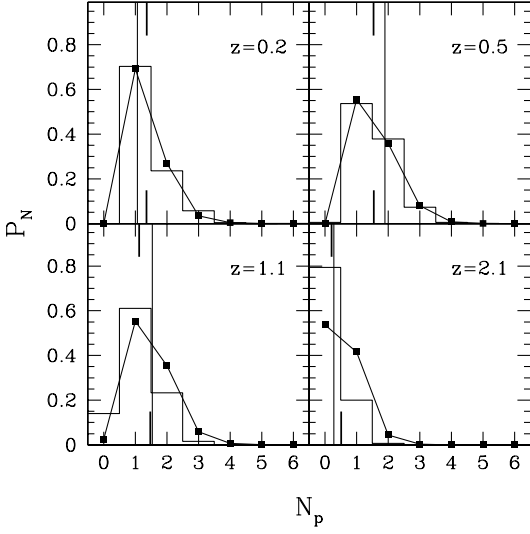


Figure 6. The probability that a halo M_0 at $z = 0$ had n progenitors, at redshifts 0.2, 0.5, 1.1, and 2.1. The square symbols show the results from the simulations, and the histogram shows the SAM-trees. The full vertical line shows the mean predicted by the EPS model. The short lines on the bottom of the boxes show the means of the simulation distributions, and the short lines on the top of the boxes show the means for the SAM-trees. top panel: $\bar{M}_0 = 10M_l$ bottom panel: $\bar{M}_0 = 40M_l$

rescaled second and third moments are the usual second and third moments divided by the first moment, such that they would be equal to unity for a Poisson distribution. Bold lines are for the SAM-trees and thin lines are for the simulations. In the first redshift step ($z = 0.2$), the moments agree at low masses ($M_0 \approx M_l$), but diverge for larger M_0 . The divergence is in the sense that the trees have a larger first, second, and third moment than the simulations. In the next redshift step, we can see the hint of the beginning of the reversal of the sense of the discrepancy, at the low M_0 end. The distribution from the SAM-trees is still somewhat broader

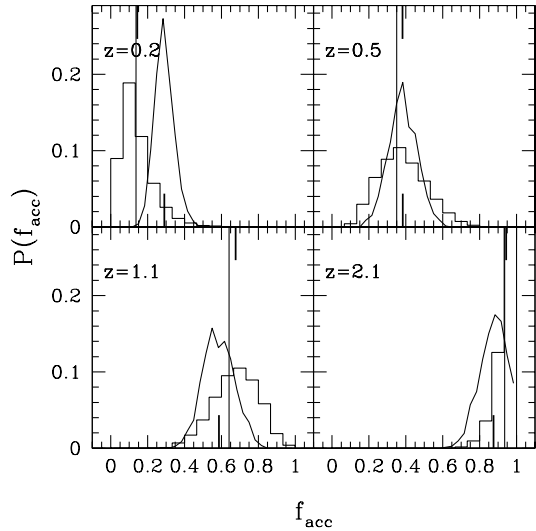
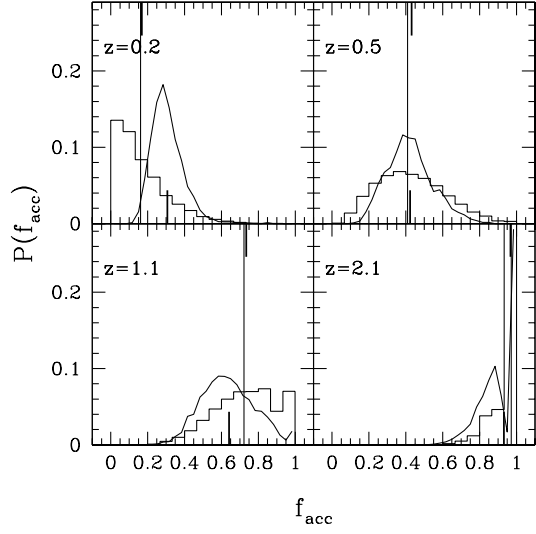


Figure 7. The probability that a fraction f_{acc} of the parent mass was in the form of accreted mass, at redshifts 0.2, 0.5, 1.1, and 2.1. The curves show the results from the simulations, and the histograms show the SAM-trees. The full vertical line shows the mean predicted by the EPS model. The short lines on the bottom of the boxes show the means of the simulation distributions (inclusive and total), and the short line on the top of the boxes shows the mean for the SAM-trees. top panel: $\bar{M}_0 = 10M_l$; bottom panel: $\bar{M}_0 = 40M_l$

(larger second moment) but now is less skewed (smaller third moment) than the simulations. The moments seem to cross on all mass scales at about $z \sim 1$ and by $z = 2$ the mean number of progenitors is *smaller* for the SAM-trees on all mass scales. The second and third moments are still larger in the trees than in the simulations.

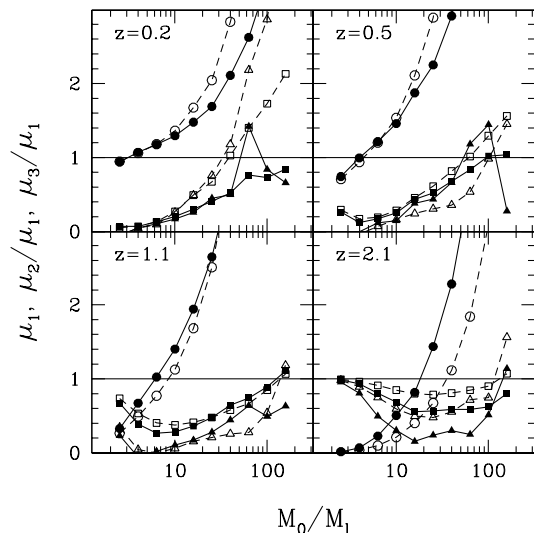


Figure 8. Moments of the distribution of the number of progenitors P_n , as a function of parent halo mass M_0 , for redshifts 0.2, 0.5, 1.1, and 2.1. Dashed lines with open symbols show the results from the SAM-trees, and solid lines with filled symbols show the results from the simulations. The dots indicate the first moment (mean), the squares the rescaled second moments (the usual second moment divided by the first moment), and the triangles the rescaled third moments (the usual third moment divided by the first moment). The rescaled moments would be equal to unity for a Poisson distribution (indicated by the horizontal line).

5.5 Largest Progenitors

A statistic which should be important in determining the properties of the galaxies that form within dark matter halos is the mass ratio of the largest and second largest progenitors. Figure 9 shows the ratio of the second largest progenitor to the largest progenitor M_2/M_1 , as a function of the ratio of the mass of the largest progenitor to the parent, M_1/M_0 . We find very good agreement between the SAM-trees and the simulations in both the mean and the variance of this quantity. Apparently, the usual discrepancy in the progenitor mass distributions cancels out. As we see from the histograms at the bottom of the figure, the mass of the largest progenitor is *larger* in the SAM-trees than in the simulations at low redshift, and *smaller* at higher redshift. This clearly follows from the original effect shown in figure 2.

6 DISCUSSION AND CONCLUSIONS

Many of the previous comparisons of the Press-Schechter model with simulations have emphasized the agreement between the two, which is surprisingly good in view of the crude assumptions underlying the model. Certainly this model has served as a useful tool in the study of structure formation. However, as comparisons of theory and observations become more refined, it is important to be aware of the limitations of the model, and to quantify its inaccuracies.

There are several implications of the errors associated with the PS and EPS model, corresponding to various im-

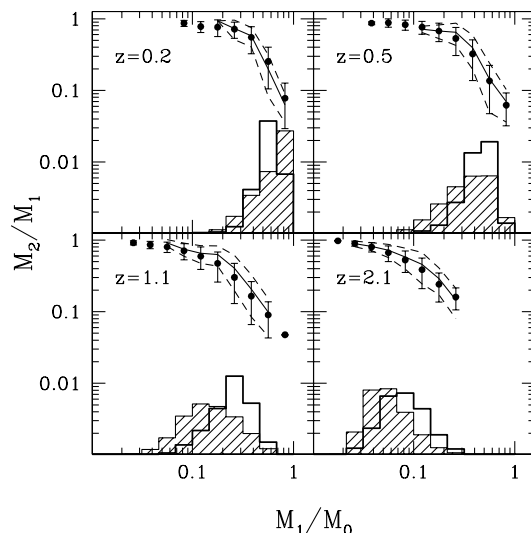
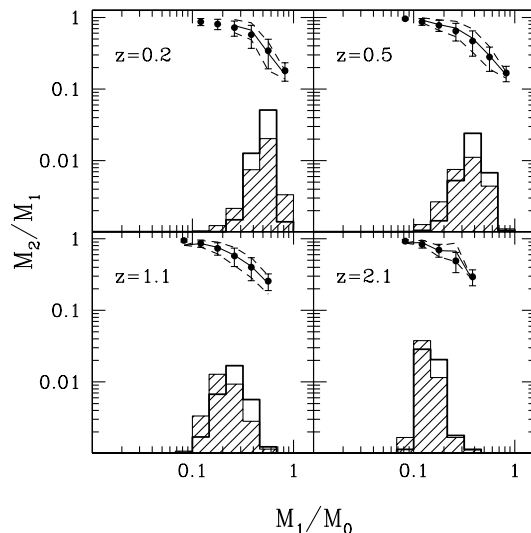


Figure 9. Masses of largest progenitors, for redshifts 0.2, 0.5, 1.1, and 2.1. The quantity plotted in the upper part of the figure is the mass ratio of the second largest to the first largest progenitor (M_2/M_1) vs. the ratio of the largest progenitor to the parent mass (M_1/M_0). Solid lines show the results from the simulations, and filled dots show the results from the SAM-trees. Dashed lines show the $1-\sigma$ variance in the simulations, and the error bars show the $1-\sigma$ variance in the SAM-trees. The histograms show the distribution of the mass of the largest progenitor. Shaded histograms are for the SAM-trees, and unshaded histograms are for the simulations.

plementations of the formalism. First, the overall abundance of halos of a given mass may be over- or underestimated by the PS model compared to N -body simulations, depending on the mass scale and the redshift. The general sense of this discrepancy is that the PS model *overestimates* the halo abundance on mass scales less than $\sim 10^{14} M_\odot$ by about a factor of 1.5 to 2.0 at $z = 0$. The model and simulation results agree well on all mass scales at an intermediate redshift

$z \sim 1$, but this agreement is momentary and fortuitous: it appears to be simply the point where the two functions happen to cross as they evolve in redshift. At higher redshifts, the abundance of large mass halos $M \gtrsim 10^{12}$ is *underestimated* by the PS model. Because this is the exponentially decreasing part of the mass function, this error can be quite serious. This behaviour seems to be qualitatively similar regardless of the cosmology or power spectrum, although the evolution with redshift (e.g. the redshift of fortuitous agreement) will be somewhat different. The precise magnitude of the discrepancy between PS and simulations depends on the cosmology, power spectrum, and the implementation of the Press-Schechter model (i.e. top-hat vs. Gaussian smoothing, value of $\delta_{c,0}$, etc.), but the dependency on mass-scale and redshift implies that the discrepancy cannot be removed by simply adjusting the parameter $\delta_{c,0}$ (see also Gross et al. 1998).

The second point is that this discrepancy is echoed qualitatively in the comparison of the conditional mass function predicted by the EPS model with the simulations. This in turn affects the predictions of merger rates, accretion rates, formation times, and the distribution of progenitor masses in merger trees based on the EPS formalism. We have shown that the distribution of the number of progenitors found in the merger trees is in fairly good agreement with the results of the simulations. On galaxy scales ($M \sim 10^{12} M_{\odot}$) these quantities are in excellent agreement. On larger mass scales ($M \sim 10^{13} M_{\odot}$, about the size of a group), the number of progenitors is over-estimated by the SAM-trees by at most a factor of two. The discrepancy increases further as the mass of the parent halo increases. This effect artificially steepens the faint-end slope of the luminosity function in EPS-based semi-analytic models of galaxy formation (e.g. Kauffmann, White, & Guiderdoni (1993), Cole et al. (1994), Somerville & Primack (1998)). This contributes to an apparent discrepancy with the observed slope, which seems to require some mechanism that strongly suppresses star formation in small-mass objects, such as strong supernovae feedback. The error resulting from the Press-Schechter model does not eliminate the need for such a mechanism but it may mean that milder, more realistic feedback will prove to be sufficient.

The two-dimensional distribution of progenitor mass and number and its evolution with redshift show the same qualitative behaviour in the SAM-trees and the simulations, although there are differences resulting directly from the discrepancies mentioned above. The second and third moments of the distribution of the number of progenitors agree fairly well, to better than a factor of two in the worst case examined here. The agreement between the first, second, and third moments of the SAM-tree and simulation distributions diverges systematically as the parent halo mass increases. The variance in the SAM-tree distributions is always larger than in the simulations. The mass ratio of the largest two progenitors, and the variance in this quantity, are in good agreement in the SAM-trees and simulations.

We have focussed on only one implementation scheme for building merger trees from the EPS theory (SK). Different schemes may yield different distribution functions for the various quantities we have presented here; however, we have argued that most of the important effects that we have discussed can be traced directly to the original EPS model and are not specific features of the merging tree scheme. We note

that our conclusions are very consistent with the findings of Kauffmann et al. (1998), who compared galaxy formation models based on a different merger-tree method (Kauffmann & White 1993) with models implemented directly within N-body simulations (the same simulations analyzed here). They note the same overall factor of two discrepancy in the halo mass function, but find that the luminosity function for a halo of a given mass is very similar in the two cases. This is presumably because, as we have noted, the relative properties of the progenitors for a halo of a given mass are in good agreement in the SAM-trees and the simulations.

Our main conclusions from this study may be summarized as follows:

- The Press-Schechter and Extended Press-Schechter models exhibit discrepancies with N-body simulations at the level of up to 50 percent. This can lead to errors in the mean numbers and masses of progenitors and the higher order moments of the progenitor number-mass distributions as well as the overall and conditional halo mass functions. More serious errors may arise at high redshifts for the rare objects at the exponentially declining high-mass end of the mass distribution (clusters). These effects must be taken into account in any detailed comparison of PS or EPS based models with observations.
- Despite these problems, *relative* properties of the progenitor distribution (such as the progenitor mass ratios) for a halo of a given mass are quite well reproduced in the merger trees, especially on galaxy mass scales. Halo merging histories constructed using the EPS formalism should thus provide a reasonably reliable framework for semi-analytic modelling of galaxy formation.

ACKNOWLEDGMENTS

The N-body simulations analysed in this paper were carried out by the Virgo Supercomputing Consortium (<http://star-www.dur.ac.uk/~frazierp/virgo/virgo.html>) using computers based at the Max-Planck-Institut für Astrophysik, Garching and the Edinburgh Parallel Computing Centre. We thank Jörg Colberg for a thorough reading of the text and helpful comments. RSS acknowledges support from an NSF GAANN fellowship. This work was supported in part by NASA ATP grant NAG5-3061 at the University of California, Santa Cruz, and by the US-Israel Binational Science Foundation grants 95-00330 and the Israel Science Foundation grant 950/95.

REFERENCES

- Bond J. R., Cole S., Efstathiou G., Kaiser N., 1991, ApJ, 379, 440
 Bower R., 1991, MNRAS, 248, 332
 Cole D., Kaiser N., 1988, MNRAS, 233, 637
 Cole S., Aragón-Salamanca A., Frenk C., Navarro J., Zepf S., 1994, MNRAS, 271, 781
 Efstathiou G., Frenk C. S., White S. D. M., Davis M., 1988, MNRAS, 235, 715
 Gelb J. M., Bertschinger E., 1994, ApJ, 436, 467
 Gross M., 1997, Ph.D. thesis, University of California, Santa Cruz, <http://fozzie.gsfc.nasa.gov>

- Gross M. A. K., Somerville R. S., Primack J. R., Holtzman J., Klypin A. A., 1998, MNRAS, submitted, astro-ph/9712142
- Jenkins A. et al., 1997, ApJ, submitted, astro-ph/9709010
- Kauffmann G., Colberg J. M., Diaferio A., White S., 1998, MNRAS, submitted, astro-ph/9805283
- Kauffmann G., White S., 1993, MNRAS, 261, 921
- Kauffmann G., White S., Guiderdoni B., 1993, MNRAS, 264, 201
- Lacey C., Cole S., 1993, MNRAS, 262, 627
- Lacey C., Cole S., 1994, MNRAS, 271, 676
- Ma C., 1996, ApJ, 471, 13
- Maddox S., Efstathiou G., Sutherland W., 1996, MNRAS, 283, 1227
- Maddox S., Efstathiou G., Sutherland W., Loveday J., 1990, MNRAS, 242, 43p
- Peebles P. J. E., 1980, *The Large-Scale Structure of the Universe*. Princeton Univ. Press, Princeton, NJ
- Press W., Schechter P., 1974, ApJ, 187, 425
- Somerville R., Kolatt T., 1998, MNRAS, in press, astro-ph/9711080 (SK)
- Somerville R., Primack J., 1998, MNRAS, submitted, astro-ph/9802268
- Tormen G., 1998, MNRAS, in press, astro-ph/9802290
- Tozzi P., Governato F., 1997, in S. D'Odorico A. F., Giallongo E., ed, *The Young Universe*. A.S.P. Conf. Ser.
- Vogele M., Park C., Geller M., Huchra J., 1992, ApJ, 391, 5